

Determining the Type, Redshift, and Phase of a Supernova Spectrum

Stéphane Blondin* and John L. Tonry†

*Harvard-Smithsonian Center for Astrophysics, Cambridge, MA 02138

†Institute for Astronomy, University of Hawaii, Honolulu, HI 96822

Abstract. We present an algorithm to identify the types of supernova spectra, and determine their redshift and phase. This algorithm, based on the correlation techniques of Tonry & Davis, is implemented in the SuperNova IDentification code (SNID). It is used by members of the ESSENCE project to determine whether a noisy spectrum of a high-redshift supernova is indeed of type Ia, as opposed to, e.g., type Ib/c. Furthermore, by comparing the correlation redshifts obtained using SNID with those determined from narrow lines in the supernova host galaxy spectrum, we show that accurate redshifts (with a typical error $\sigma_z \lesssim 0.01$) can be determined for SNe Ia for which a spectrum of the host galaxy is unavailable. Last, the phase of an input spectrum is determined with a typical accuracy of $\sigma_t \lesssim 3$ days.

Keywords: methods: data analysis — methods: statistical — supernovae: general

PACS: 95.75.-z, 95.75.Fg, 95.75.Pq, 97.60.Bw, 98.52.Cf, 98.62.Py, 98.80.Es

INTRODUCTION

Supernovae play a major role in the recent revival of observational cosmology. It is through observations of type-Ia supernovae (SNe Ia) over a large redshift range that two teams were able to independently confirm the present accelerated rate of the universal expansion [1, 2]. This astonishing result has been confirmed in subsequent years at moderate redshifts [3, 4, 5], but also at higher ($z > 1$) redshifts where the universal expansion is in a decelerating phase [6]. Currently, two ongoing projects have the more ambitious goal to measure the equation-of-state parameter of the “dark energy” that drives the expansion: the ESSENCE [7] and SNLS [8] projects. The success of these cosmological experiments depends, amongst other things, on the assurance that the supernovae in the sample are of the correct type, namely, SNe Ia. Inclusion of supernovae that are of a different type or exclusion of SNe Ia from the sample leads to biased cosmological parameters in the former case [9] and increased statistical errors on these same parameters in the latter. The secure classification of supernovae is a challenge at all redshifts, however. Even with high signal-to-noise ratio (S/N) spectra, the distinction between supernova of different types (or between subtypes within a given type) can pose problems.

The spectrum of a supernova also contains information on its redshift and phase. Knowledge of the SN redshift is necessary for the use of SNe Ia as distance indicators (though see [10] for redshift-independent distances), and is usually determined *via* narrow lines in the spectrum of the host galaxy. When such a spectrum is unavailable, however, one has to rely on comparison with SN template spectra for determining the redshift. The SN phase is usually determined using a well-sampled lightcurve, but a

single spectrum can also provide a relatively accurate estimate. Moreover, comparison of spectral and lightcurve phases of high-redshift supernovae can be used to test the general relativistic prediction of time dilation [11, 12].

We have developed a tool (SuperNova IDentification; SNID) to determine the type, redshift and phase of a supernova, using a single spectrum. The algorithm is based on the correlation techniques of Tonry & Davis [13], and relies on the comparison of an input spectrum with a database of high-S/N template spectra. Our database presently comprises 796 spectra of 64 SNe Ia, 172 spectra of 8 SNe Ib, 116 spectra of 9 SNe Ic, 353 spectra of 10 SNe II, as well as spectra of galaxies, AGNs, and variable stars. The supernova spectra cover a broad range of phases, and span a sufficient restframe wavelength range ($\lambda_{\min} \leq 4000 \text{ \AA}$; $\lambda_{\max} \geq 6500 \text{ \AA}$) to include all the identifying features of SN spectra. Most of these spectra are publicly available through the SUSPECT¹ and CfA² SN spectral archives.

We briefly describe the cross-correlation technique in the next section, and then test the accuracy of correlation redshifts and phases using SNID. Last, we tackle the issue of supernova classification by focusing on two examples relevant to SN searches at high redshifts.

CROSS-CORRELATION TECHNIQUES

The cross-correlation method presented here is extensively discussed by Tonry and Davis [13], where it is exclusively applied to galaxy spectra. Nonetheless, the formalism is easy to adapt to supernova spectra. The correlation technique is in principle fairly straightforward: a supernova spectrum, $s(n)$, whose redshift, z , is to be found is cross-correlated with a template spectrum, $t(n)$ (of known type and phase) at zero redshift. We want to determine the $(1+z)$ wavelength scaling, that maximizes the cross-correlation $c(n) = s(n) \star t(n)$. In practice, it is convenient to bin the spectra linearly with $\ln \lambda$, where λ denotes the wavelength. Scaling the wavelength axis of $t(n)$ by a factor $(1+z)$ is then equivalent to adding a $\ln(1+z)$ shift to the logarithmic wavelength axis of $t(n)$, i.e. a (velocity) redshift corresponds to a uniform linear shift.

We show the result of mapping an input supernova spectrum onto a logarithmic wavelength axis in Fig. 1. We show the input spectrum in panel (a) and its $\ln \lambda$ binned version in panel (b). The next step in preparing the spectra for correlation analysis is *pseudo*-continuum subtraction ([13]; Fig. 1, panel (c)). The purpose is to effectively remove any intrinsic color information in the input and template spectra, and to ensure the correlation is not affected by reddening uncertainties or instrumental distortions. This effectively discards any spectral color information, and the correlation only relies on the *relative* shape and strength of spectral features in the input and template spectra. The final step is the application of a bandpass filter (Fig. 1, panel (d)). The goal is to remove low-frequency residuals left over from the pseudo-continuum subtraction and high-frequency noise components.

¹ <http://bruford.nhn.ou.edu/~suspect/index1.html>

² <http://www.cfa.harvard.edu/oir/Research/supernova/SNarchive.html>

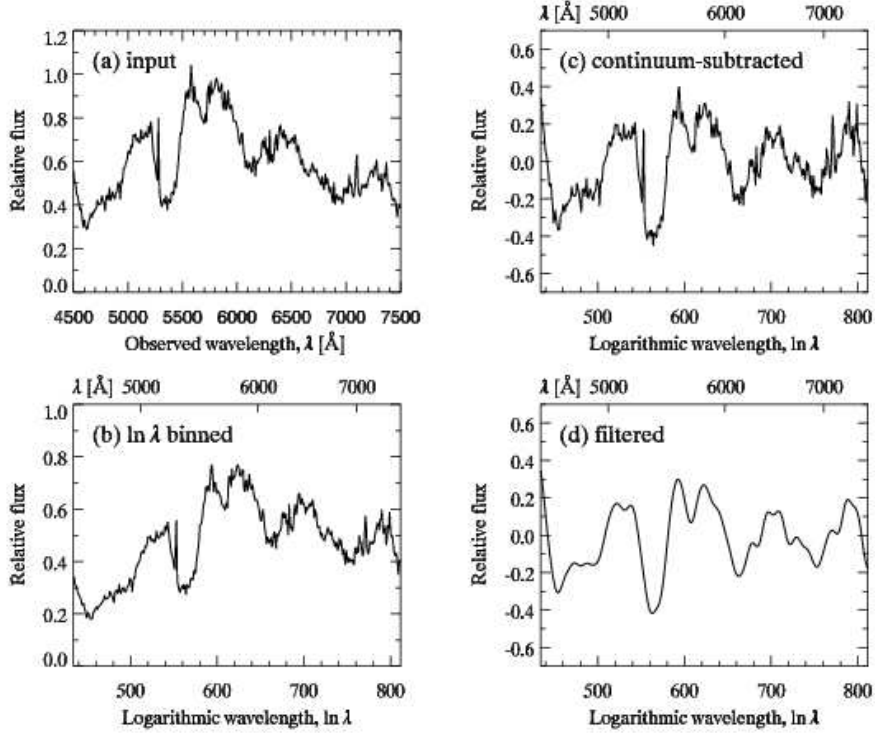


FIGURE 1. Spectrum pre-processing. The input spectrum (a) is binned on a logarithmic wavelength scale (b). A *pseudo*-continuum is subtracted (c) and the resulting spectrum is bandpass filtered (d).

Tonry and Davis [13] introduce a parameter, r , to quantify the significance of a correlation peak in $c(n)$. It is defined as the ratio of the height h of the peak to the root-mean-square (RMS), σ_a , of the antisymmetric component of $c(n)$ about the correlation redshift (see Fig. 2). A perfect correlation will have a peak with $h = 1$ at the exact redshift, and $c(n)$ will be symmetric about this redshift, i.e. $\sigma_a = 0$ and $r \rightarrow \infty$. Conversely, r will be small ($r < 3$) for a spurious correlation peak, and large ($r \gtrsim 8$) for a significant peak, since h will be close to 1 and σ_a will be small. The width of the correlation peak, w , is used to formally evaluate the redshift error (not discussed here).

The r -value is further weighted by the overlap in $\ln \lambda$ space (at the correlation redshift) between the input spectrum and each of the template spectra used in the correlation. The template spectra are trimmed to match the wavelength range of the input spectrum at the redshift corresponding to the correlation peak. The overlap value, lap , conveys important absolute information about the quality of the correlation, complementary to the correlation parameter r . We usually discard correlation redshifts that have an associated $lap < lap_{\min} = 0.40$ and a combined $rlap = r \times lap < rlap_{\min} = 5$.

REDSHIFT AND PHASE DETERMINATION

We use a simple simulation to test the accuracy of SNID in determining the redshift and phase of a supernova spectrum. Here we only consider “normal” type-Ia supernovae

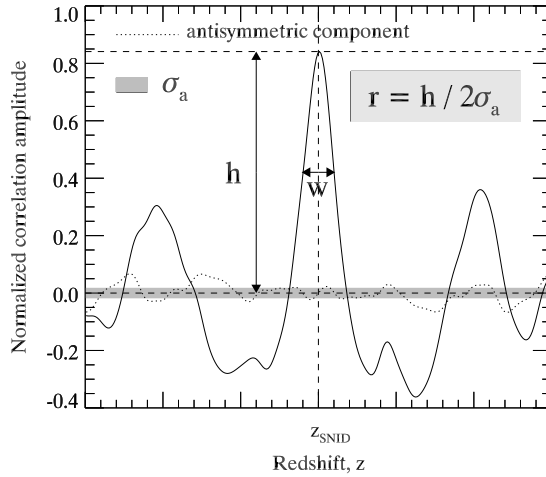


FIGURE 2. The correlation r -value is defined as the ratio of the height, h , of the highest peak in the normalized correlation function (*solid line*) to twice the RMS, σ_a , of its antisymmetric component (*dotted line*).

since they are the most represented in our spectral database, though the conclusions announced in this section are qualitatively valid for all other supernova types.

In this simulation, each normal SN Ia spectrum in the database is correlated with all other normal SN Ia spectrum using SNID, after having taken care to temporarily remove all spectra corresponding to the input supernova from the database. The input spectrum is first redshifted at random in the interval $0.1 \leq z \leq 0.7$. We then add noise (both random Poisson noise and sky background) to reproduce the range of typical signal-to-noise ratio of SN spectra at the simulation redshifts, when observed with 8-10 m-class telescopes (e.g., VLT, Keck, Gemini) used in cosmological SN Ia surveys.

We show the distribution of redshift residuals, Δz vs. the $rlap$ parameter in the upper panel of Fig. 3, for input spectra satisfying $0.3 \leq z \leq 0.5$; $-5 \leq t$ [days] $\leq +15$ (t is the SN phase); $2 \leq S/N$ (per \AA) ≤ 10 . The residuals are shown as a two-dimensional histogram, with a grayscale scheme reflecting the number of points in a given $[\Delta z, rlap]$ 2D bin (darker for more points). We only show correlations for which the overlap between input and template spectra $lap \geq 0.40$. For good correlations ($rlap \gtrsim 5$), the distribution of redshift residuals is a Gaussian centered at $\Delta z = 0$. In the lower panel, we show the standard deviation of redshift residuals, σ_z , in $rlap$ bins of size unity. For $rlap \gtrsim 5$, we have a typical error in redshift of order $\sigma_z \lesssim 0.01$.

For poor correlations ($rlap \lesssim 3$) there is a concentration of points around $\Delta z \approx -0.01$. This is due to the SN Ia template phase distribution in our database: many input spectra at post-maximum phases ($t \lesssim +10$ days) are attracted to higher phases ($\gtrsim +10$ days), where the position of SN spectral features has shifted redward in wavelength due to the expansion of the supernova envelope. The template needs to be shifted less in $\ln \lambda$ space to match the redshift of the input spectrum, which leads to an under-estimation of the redshift (by ~ 0.01) corresponding to a combination of the typical velocity shift in SN Ia absorption features from maximum to ~ 10 days past maximum, and the spread of these

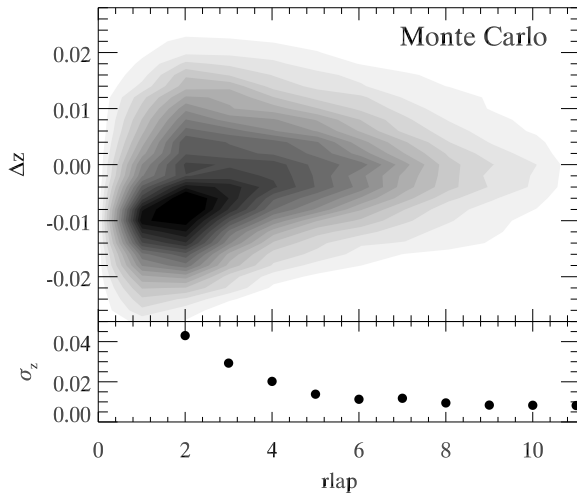


FIGURE 3. *Upper panel:* Redshift residuals vs. $rlap$. *Lower panel:* Standard deviation of redshift residuals in $rlap$ bins of size unity. For $rlap \gtrsim 5$, $\sigma_z \lesssim 0.01$.

velocities at a given phase for different supernovae ($\sim 3000 \text{ km s}^{-1}$; see [14, 15]).

This covariance between redshift and phase (over-estimating the phase leads to under-estimating the redshift, and *vice versa*) suggests that priors on one parameter should improve the accuracy of the other. Fig. 4 shows the effect on the distributions phase residuals (for $rlap \geq 5$) of adding a flat ± 0.01 prior on redshift. As expected, a prior on redshift slightly improves the phase determination ($\sigma_t = 3.4$ days to $\sigma_t = 2.9$ days). A flat ± 3 -day prior also improves the redshift determination ($\sigma_z = 0.006$ to $\sigma_z = 0.004$, not shown here). In practice, the prior on redshift generally comes from a spectrum of the SN host galaxy, and one can impose a prior on phase if a well-sampled lightcurve of the supernova (i.e. one for which the date of maximum light is easily determined) is available.

We test the accuracy of correlation redshifts using SNID by comparing it with that obtained from narrow emission/absorption lines in the host galaxy spectrum. We have selected high-redshift SN Ia spectra taken by members of the ESSENCE team [16, 17], for which a redshift of the host galaxy could be obtained. This amounts to 47 SN Ia spectra in the redshift range $0.164 \leq z \leq 0.781$. The result of this comparison is shown in Fig. 5. The upper panel is a plot of the supernova redshift determined *via* cross-correlation using SNID, *vs.* that determined from narrow lines in the host galaxy spectrum. The dispersion about the one-to-one correspondence of the redshifts is excellent, with $\sigma \approx 0.006$ over the whole redshift range. This is in good agreement with the expected redshift residual found from simulations. The lower panel shows a plot of the redshift residuals as a function of the galaxy redshift.

TYPE DETERMINATION

The previous results are only valid if we assume we know the type of the input supernova spectrum— in this case a “normal” SN Ia. Although SNID is tuned to determining SN

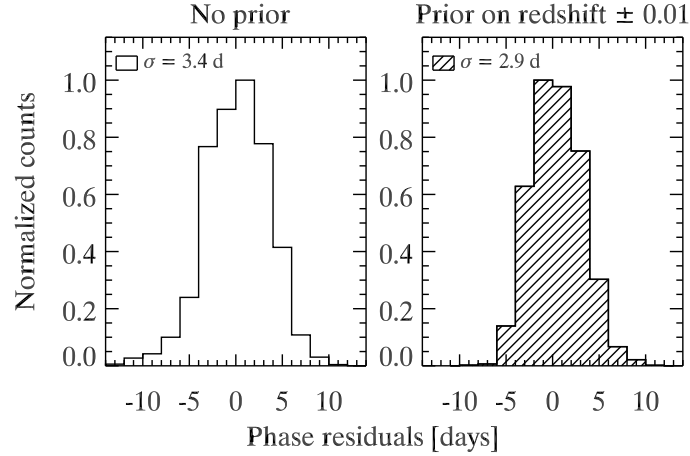


FIGURE 4. Effect of a redshift prior on the phase determination. With no redshift prior (*right*), $\sigma_t = 3.4$ days. With a flat ± 0.01 redshift prior, $\sigma_t = 2.9$ days.

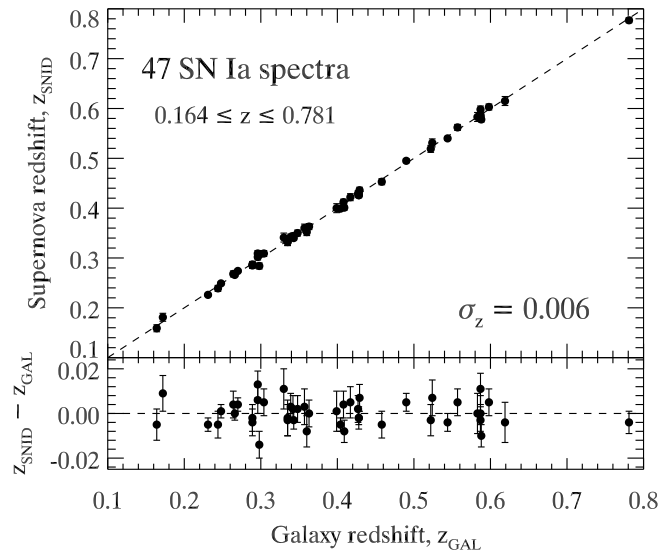


FIGURE 5. *Upper panel:* Comparison of redshifts determined from cross-correlations with SN Ia templates using SNID (z_{SNID}) and from narrow lines in the host galaxy spectrum (z_{GAL}). The dispersion about the one-to-one correspondence is $\sigma_z \approx 0.006$ over the redshift range $0.164 \leq z \leq 0.781$. *Lower panel:* Redshift residuals vs. z_{GAL} . The data are from the ESSENCE project [16, 17].

redshifts, we investigate its potential in assigning a probability to the input spectrum being of a certain type. We focus on two distinct examples, particularly relevant to ongoing high-redshift SN Ia searches: the distinction between 1991T-like SNe Ia and other type-Ia supernovae, and the increasing difficulty to distinguish between type-Ic supernovae and SNe Ia at high redshifts.

It can be a challenge to distinguish the subtypes of SNe Ia from one another (Fig. 6, *right*). 1991T-like SNe Ia supernovae have a peak luminosity at the bright end of the

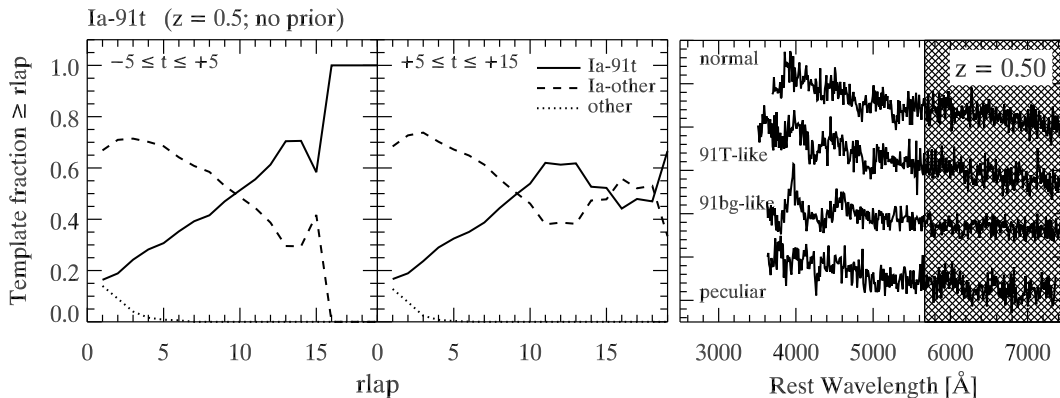


FIGURE 6. Identification of a 1991T-like SN Ia at $z = 0.5$, around maximum light (*right*) and past maximum light (*middle*). The curves correspond to the fraction of templates of a given type greater than a given $rlap$ value: 1991T-like SNe Ia (*solid*); other SNe Ia (*dashed*); other SN types (*dotted*). The left panel shows representative maximum-light spectra of the various SN Ia subtypes, as observed with a typical optical spectrograph at $z = 0.5$. Note that the relative differences in *pseudo*-continuum shapes has no impact on the SNID results.

SN Ia distribution, and although their lightcurves still obey the Phillips relation [18], it is useful to have an independent confirmation of their high intrinsic luminosity *via* their spectra. Spectra of 1991T-like SNe Ia are characterized by the near-absence of Ca II and Si II lines in the early-time spectra, and prominent high-excitation features of Fe III— not found in “normal” SNe Ia. The Si II, S II, and Ca II features develop during the post-maximum phases, and by ~ 2 weeks past maximum the spectra of “1991T-like” objects are similar to those of “normal” SNe Ia.

In Fig. 6 (*left*) we illustrate the ability for SNID to identify 1991T-like SNe Ia around maximum light (i.e. when the spectroscopic differences with “normal” SNe Ia are most apparent) at $z = 0.5$. We show the fraction of templates in the SNID database that correlate with the input spectrum, as a function of the $rlap$ parameter: 1991T-like SNe Ia (*solid line*); other SNe Ia (*dashed line*); supernovae of other types (*dotted line*). For $rlap \gtrsim 10$, the fraction of 1991T-like templates dominates over the other SN Ia subtypes. The confusion with other SN types is always low and inexistent for $rlap > 5$. At $\sim 1 - 2$ weeks past maximum light, however, the distinction is more difficult to make (as expected) with roughly a 50% probability to recover another SN Ia subtype (Fig. 6, *middle*).

The mis-identification of supernovae of other types as SNe Ia is a major concern for ongoing high-redshift SN Ia searches (Fig. 7, *right*). Including only a small fraction non-Ia supernovae in a sample will lead to a mis-calibration of the absolute magnitudes of these objects, and to biases in the derived cosmological parameters [9]. A particular concern is the contamination of high- z SN Ia samples with type-Ic supernovae. At redshifts $z \gtrsim 0.4$, the defining Si II $\lambda 6355$ absorption feature of SNe Ia (also present, though somewhat weaker, in SNe Ic) is redshifted out of the range of most optical spectrographs, and one has to rely on spectral features blueward of this to determine the supernova type. Some of these features, such as the Ca II H&K $\lambda\lambda 3934, 3968$ doublet, are common to both SNe Ia and SNe Ic. Other features characteristic of SN Ia spectra

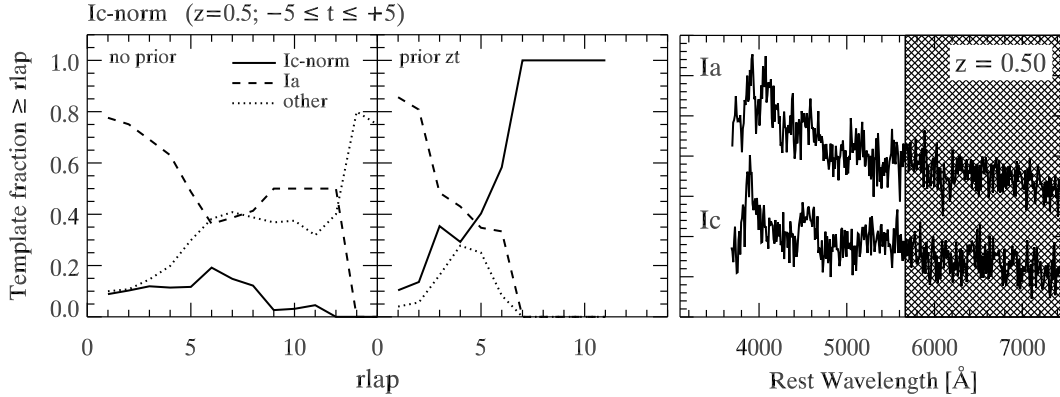


FIGURE 7. Identification of a normal SN Ic around maximum light at $z = 0.5$, with no prior on redshift or phase (*right*), and with a flat ± 0.01 prior on redshift and a ± 3 -day prior on the phase (*middle*). The curves correspond to the fraction of templates of a given type greater than a given $rlap$ value: normal SNe Ic (*solid*); SNe Ia (*dashed*); other SN types (*dotted*). The left panel shows representative maximum-light spectra of SNe Ia and SNe Ic, as observed with a typical optical spectrograph at $z = 0.5$. Note that the relative differences in *pseudo*-continuum shapes has no impact on the SNID results.

around maximum light (e.g. S II $\lambda\lambda 5454, 5640$) are generally weak and can be difficult to detect in low-S/N spectra. One has to invoke external constraints, such as the SN color evolution, lightcurve shape, host galaxy morphology (only SNe Ia occur in early-type hosts; [19]), or the expected apparent peak magnitude: type-Ic supernovae at maximum light are often $\gtrsim 1$ mag fainter than SNe Ia, and hence are not expected to pollute magnitude-limited samples of SNe Ia at high redshift (although Clocchiatti et al. 20 have reported on a type-Ic SN with a similar absolute magnitude as normal SNe Ia).

In Fig. 7 (*left*) we illustrate the ability for SNID to identify SNe Ic around maximum light ($-5 \leq t$ [days] $\leq +5$) at $z = 0.5$. We show the fraction of templates in the SNID database that correlate with the input spectrum, as a function of the $rlap$ parameter: “normal” SNe Ic (*solid line*); SNe Ia (*dashed line*); supernovae of other types (*dotted line*). For “good” correlations ($rlap \geq 5$), the input spectrum almost always correlates with supernovae of other types. With an additional flat ± 0.01 prior on redshift and a flat ± 3 -day prior on the phase, the fraction of SN Ic templates dominates for $rlap \gtrsim 5$ (Fig. 7, *middle*). In the absence of such priors, one needs to invoke non-spectral constraints on the type to identify potential SN Ic contaminants in high-redshift SN Ia samples.

CONCLUSION AND FUTURE WORK

We have presented an algorithm, based on the correlation techniques of Tonry & Davis [13], which can be used to determine the redshift and phase of a supernova spectrum and place constraints on its type. We develop a diagnostic, the $rlap$ parameter, to quantify the quality of a given correlation between the input and a template spectrum. This parameter is simply the product of the Tonry & Davis r -value and the overlap, lap , in $\ln \lambda$ space between the input and template spectrum at the correlation redshift. We show, based

on simulations, that for $rlap \gtrsim 5$, the typical error on redshift and phase is $\sigma_z \lesssim 0.01$ and $\sigma_t \lesssim 3$ days, respectively. The former accuracy on redshift is confirmed through a comparison of correlation redshifts with host-galaxy redshifts (determined from narrow lines in the spectrum) out to redshifts $z \lesssim 0.8$.

We present first results of an impartial and effective spectroscopic classification of supernovae, based on the cumulative fraction of correlations exceeding a certain $rlap$ cutoff. We illustrate this through two examples, relevant to ongoing SN Ia searches at high redshift: we are able to distinguish 1991T-like SNe Ia from other SNe Ia at $z = 0.5$, if the input spectrum is within five days from maximum light; we identify a type-Ic supernova as such at $z = 0.5$, but only when an additional prior on redshift and phase is applied. These examples both illustrate the success and limitations of such an automated classification scheme, and highlight the complementarity between spectroscopic and photometric observations in determining the supernova type.

The current version of SNID will soon be made available to the community, and we plan to set up a web-based interface for instantaneous supernova typing (and redshift/phase determination). Future versions of SNID will include a wavelength-weighted lap parameter, an explicit treatment of the covariance between redshift and phase, and a Bayesian approach to type determination, as currently used for photometric classification of supernovae [21, 22]. Moreover, more spectral templates are continuously being included in the SNID database, which directly impact the ability for SNID to securely identify input spectra.

ACKNOWLEDGMENTS

This work has been funded in part by the US National Science Foundation through grants AST 0443378, AST 057475, and AST 0606772. This research has made use of the CfA Supernova Archive, which is funded in part by the National Science Foundation through grant AST 0606772.

REFERENCES

1. A. G. Riess, A. V. Filippenko, P. Challis, A. Clocchiatti, A. Diercks, P. M. Garnavich, R. L. Gilliland, C. J. Hogan, S. Jha, R. P. Kirshner, B. Leibundgut, M. M. Phillips, D. Reiss, B. P. Schmidt, R. A. Schommer, R. C. Smith, J. Spyromilio, C. Stubbs, N. B. Suntzeff, and J. Tonry, *AJ* **116**, 1009–1038 (1998), [astro-ph/9805201](#).
2. S. Perlmutter, G. Aldering, G. Goldhaber, R. A. Knop, P. Nugent, P. G. Castro, S. Deustua, S. Fabbro, A. Goobar, D. E. Groom, I. M. Hook, A. G. Kim, M. Y. Kim, J. C. Lee, N. J. Nunes, R. Pain, C. R. Pennypacker, R. Quimby, C. Lidman, R. S. Ellis, M. Irwin, R. G. McMahon, P. Ruiz-Lapuente, N. Walton, B. Schaefer, B. J. Boyle, A. V. Filippenko, T. Matheson, A. S. Fruchter, N. Panagia, H. J. M. Newberg, W. J. Couch, and The Supernova Cosmology Project, *ApJ* **517**, 565–586 (1999), [astro-ph/9812133](#).
3. J. L. Tonry, B. P. Schmidt, B. Barris, P. Candia, P. Challis, A. Clocchiatti, A. L. Coil, A. V. Filippenko, P. Garnavich, C. Hogan, S. T. Holland, S. Jha, R. P. Kirshner, K. Krisciunas, B. Leibundgut, W. Li, T. Matheson, M. M. Phillips, A. G. Riess, R. Schommer, R. C. Smith, J. Sollerman, J. Spyromilio, C. W. Stubbs, and N. B. Suntzeff, *ApJ* **594**, 1–24 (2003), [astro-ph/0305008](#).
4. R. A. Knop, G. Aldering, R. Amanullah, P. Astier, G. Blanc, M. S. Burns, A. Conley, S. E. Deustua, M. Doi, R. Ellis, S. Fabbro, G. Folatelli, A. S. Fruchter, G. Garavini, S. Garmond, K. Garton,

- R. Gibbons, G. Goldhaber, A. Goobar, D. E. Groom, D. Hardin, I. Hook, D. A. Howell, A. G. Kim, B. C. Lee, C. Lidman, J. Mendez, S. Nobili, P. E. Nugent, R. Pain, N. Panagia, C. R. Penny-packer, S. Perlmutter, R. Quimby, J. Raux, N. Regnault, P. Ruiz-Lapuente, G. Sainton, B. Schaefer, K. Schahmaneche, E. Smith, A. L. Spadafora, V. Stanishev, M. Sullivan, N. A. Walton, L. Wang, W. M. Wood-Vasey, and N. Yasuda, *ApJ* **598**, 102–137 (2003), [astro-ph/0309368](#).
5. B. J. Barris, J. L. Tonry, S. Blondin, P. Challis, R. Chornock, A. Clocchiatti, A. V. Filippenko, P. Garnavich, S. T. Holland, S. Jha, R. P. Kirshner, K. Krisciunas, B. Leibundgut, W. Li, T. Matheson, G. Miknaitis, A. G. Riess, B. P. Schmidt, R. C. Smith, J. Sollerman, J. Spyromilio, C. W. Stubbs, N. B. Suntzeff, H. Aussel, K. C. Chambers, M. S. Connelley, D. Donovan, J. P. Henry, N. Kaiser, M. C. Liu, E. L. Martín, and R. J. Wainscoat, *ApJ* **602**, 571–594 (2004), [astro-ph/0310843](#).
 6. A. G. Riess, L.-G. Strolger, J. Tonry, S. Casertano, H. C. Ferguson, B. Mobasher, P. Challis, A. V. Filippenko, S. Jha, W. Li, R. Chornock, R. P. Kirshner, B. Leibundgut, M. Dickinson, M. Livio, M. Giavalisco, C. C. Steidel, T. Benítez, and Z. Tsvetanov, *ApJ* **607**, 665–687 (2004), [astro-ph/0402512](#).
 7. W. M. Wood-Vasey et al., *ApJ*, *submitted* (2007).
 8. P. Astier, J. Guy, N. Regnault, R. Pain, E. Aubourg, D. Balam, S. Basa, R. G. Carlberg, S. Fabbro, D. Fouchez, I. M. Hook, D. A. Howell, H. Lafoux, J. D. Neill, N. Palanque-Delabrouille, K. Perrett, C. J. Pritchet, J. Rich, M. Sullivan, R. Taillet, G. Aldering, P. Antilogus, V. Arsenijevic, C. Balland, S. Baumont, J. Bronder, H. Courtois, R. S. Ellis, M. Filiol, A. C. Gonçalves, A. Goobar, D. Guide, D. Hardin, V. Lussat, C. Lidman, R. McMahon, M. Mouchet, A. Mourao, S. Perlmutter, P. Ripoché, C. Tao, and N. Walton, *A&A* **447**, 31–48 (2006), [astro-ph/0510447](#).
 9. N. L. Homeier, *ApJ* **620**, 12–20 (2005), [astro-ph/0410593](#).
 10. B. J. Barris, and J. L. Tonry, *ApJL* **613**, L21–L24 (2004), [astro-ph/0408097](#).
 11. A. G. Riess, A. V. Filippenko, D. C. Leonard, B. P. Schmidt, N. Suntzeff, M. M. Phillips, R. Schommer, A. Clocchiatti, R. P. Kirshner, P. Garnavich, P. Challis, B. Leibundgut, J. Spyromilio, and R. C. Smith, *AJ* **114**, 722–729 (1997), [astro-ph/9707260](#).
 12. R. J. Foley, A. V. Filippenko, D. C. Leonard, A. G. Riess, P. Nugent, and S. Perlmutter, *ApJL* **626**, L11–L14 (2005), [astro-ph/0504481](#).
 13. J. Tonry, and M. Davis, *AJ* **84**, 1511–1525 (1979).
 14. S. Benetti, E. Cappellaro, P. A. Mazzali, M. Turatto, G. Altavilla, F. Bufano, N. Elias-Rosa, R. Kotak, G. Pignata, M. Salvo, and V. Stanishev, *ApJ* **623**, 1011–1016 (2005), [astro-ph/0411059](#).
 15. S. Blondin, L. Dessart, B. Leibundgut, D. Branch, P. Höflich, J. L. Tonry, T. Matheson, R. J. Foley, R. Chornock, A. V. Filippenko, J. Sollerman, J. Spyromilio, R. P. Kirshner, W. M. Wood-Vasey, A. Clocchiatti, C. Aguilera, B. Barris, A. C. Becker, P. Challis, R. Covarrubias, T. M. Davis, P. Garnavich, M. Hicken, S. Jha, K. Krisciunas, W. Li, A. Miceli, G. Miknaitis, G. Pignata, J. L. Prieto, A. Rest, A. G. Riess, M. E. Salvo, B. P. Schmidt, R. C. Smith, C. W. Stubbs, and N. B. Suntzeff, *AJ* **131**, 1648–1666 (2006), [astro-ph/0510089](#).
 16. T. Matheson, S. Blondin, R. J. Foley, R. Chornock, A. V. Filippenko, B. Leibundgut, R. C. Smith, J. Sollerman, J. Spyromilio, R. P. Kirshner, A. Clocchiatti, C. Aguilera, B. Barris, A. C. Becker, P. Challis, R. Covarrubias, P. Garnavich, M. Hicken, S. Jha, K. Krisciunas, W. Li, A. Miceli, G. Miknaitis, J. L. Prieto, A. Rest, A. G. Riess, M. E. Salvo, B. P. Schmidt, C. W. Stubbs, N. B. Suntzeff, and J. L. Tonry, *AJ* **129**, 2352–2375 (2005), [astro-ph/0411357](#).
 17. R. J. Foley et al., *in prep* (2007).
 18. M. M. Phillips, *ApJL* **413**, L105–L108 (1993).
 19. E. Cappellaro, M. Turatto, D. Y. Tsvetkov, O. S. Bartunov, C. Pollas, R. Evans, and M. Hamuy, *A&A* **322**, 431–441 (1997), [astro-ph/9611191](#).
 20. A. Clocchiatti, M. M. Phillips, N. B. Suntzeff, M. DellaValle, E. Cappellaro, M. Turatto, M. Hamuy, R. Avilés, M. Navarrete, C. Smith, E. P. Rubenstein, R. Covarrubias, P. B. Stetson, J. Maza, A. G. Riess, and C. Zanin, *ApJ* **529**, 661–674 (2000), [astro-ph/9909058](#).
 21. D. Poznanski, D. Maoz, and A. Gal-Yam (2006), [astro-ph/0610129](#).
 22. N. V. Kuznetsova, and B. M. Connolly (2006), [astro-ph/0609637](#).